Enhancement of near-cloaking. Part III: Numerical simulations, statistical stability, and related questions*

Habib Ammari† Josselin Garnier‡ Vincent Jugnon§ Hyeonbae Kang¶
Hyundae Lee¶ Mikyoung Lim‖

December 26, 2011

Abstract

The goal of this paper is to illustrate the efficiency and the stability of the near-cloaking structures proposed in [4] and [5]. These new structures are, before using transformation optics, layered structures and are designed so that their first contracted generalized polarization tensors (in the quasi-static limit) or scattering coefficients (in the case of the Helmholtz equation) vanish. Inside the cloaking region, any target has near-zero boundary or scattering cross section measurements. We numerically show that this new construction significantly enhances the invisibility cloaking effect for the conductivity and the Helmholtz equations and is quite robust with respect to random fluctuations of the material parameters around their theoretical values. We finally extend our multi-coated construction to the enhanced reshaping problem. We show how to make any target look like a disc with homogeneous physical parameters.

AMS subject classifications. 35R30, 35B30

Key words. cloaking, reshaping, transformation optics, conductivity problem, Helmholtz equation, Dirichlet-to-Neumann map, boundary measurements, scattering cross section, contracted generalized polarization tensors, scattering coefficients

1 Introduction

The cloaking problem is to make a target invisible from far-field wave measurements [22, 15, 10, 9, 16, 18]. Many schemes are under active current investigation. These include exterior cloaking in which the cloaking region is outside the cloaking device [19, 20, 8, 7, 2, 1], active cloaking [11], and interior cloaking, which is the focus of our study.

In interior cloaking, the difficulty is to construct material parameter distributions of a cloaking structure such that any target placed inside the structure is undetectable to waves. One approach is to use transformation optics [22, 10, 9, 27, 12, 23]. It takes advantage of the fact that the equations governing electrostatics, electromagnetism, and acoustics have transformation laws under change of variables. This allows one to design structures that steel waves around a hidden region, returning

*This work was supported by ERC Advanced Grant Project MULTIMOD–267184 and National Research Foundation of Korea through grants No. 2010-0017532, 2010-0004091, and 2009-0090250.

†Department of Mathematics and Applications, Ecole Normale Supérieure, 45 Rue d'Ulm, 75005 Paris, France (habib.ammari@ens.fr).

‡Laboratoire de Probabilités et Modèles Aléatoires & Laboratoire Jacques-Louis Lions, Université Paris VII, 2 Place Jussieu, 75251 Paris Cedex 5, France (garnier@math.jussieu.fr).

§Department of Mathematics, Massachusetts Institute of Technology, 77 Massachusetts Avenue, Cambridge, MA 02139-4307, USA (vjugnon@math.mit.edu).

¶Department of Mathematics, Inha University, Incheon 402-751, Korea (hbkang@inha.ac.kr, hdlee@inha.ac.kr).

‖Department of Mathematical Sciences, Korean Advanced Institute of Science and Technology, Daejeon 305-701, Korea (mklim@kaist.ac.kr).

them to their original path on the far side. The change of variables based cloaking method uses a singular transformation to boost the material properties so that it makes a cloaking region look like a point to outside measurements. However, this transformation induces the singularity of material constants in the transversal direction (also in the tangential direction in two dimensions), which causes difficulty both in the theory and applications. To overcome this weakness, so called 'near cloaking' is naturally considered, which is a regularization or an approximation of singular cloaking. In [14], instead of the singular transformation, the authors use a regular one to push forward the material constant in the conductivity equation describing the static limit of electromagnetism, in which a small ball is blown up to the cloaking region. In [13], this regularization point of view is adopted for the Helmholtz equation. See also [17, 21].

In [4, 5], a new cancellation technique in order to achieve enhanced invisibility from measurements of the Dirichlet-to-Neumann map in electrostatics and the scattering cross section in electromagnetism is proposed. The approach is to first design a multi-coated structure around a small perfect insulator to significantly reduce its effect on boundary or scattering cross section measurements. One then obtains near-cloaking structure by pushing forward the multi-coated structure around a small object via the standard blow-up transformation technique.

The purpose of this paper is to study the performances of the invisibility cloaks proposed in [4] and [5], and compare them with those based on (regularized) transformation optics [14, 13]. We show that they are quite robust with respect to random fluctuations of their material parameters around the theoretical values. We also extend the new construction in [4] and [5] to reshaping problems.

Practical performances of cloaks can be evaluated in terms of invisibility and complexity. Invisibility tells how difficult it is to detect the cloaked object. Complexity reflects how difficult it is to produce the cloak in practice. It takes into account possible singularities, high or low values, and anisotropy of the parameter distributions.

The approach developed in [4] and [5] is to drastically reduce the visibility of an object by making contracted generalized polarization tensors (GPT) or scattering coefficients of the multi-coated structure vanish (up to some order). This is achieved using a properly designed layered-structure, combined with the usual change of variable. To compare (in)visibility, we use scalar functions. For the conductivity problem, we choose the eigenvalues of the Dirichlet-to-Neumann map which are linked to the contracted generalized polarization tensors. Similarly, for the Helmholtz problem, we consider the singular values of the far-field operator which are functions of the scattering coefficients. Given bounded material properties and a finite signal-to-noise ratio, we show that the new structures proposed in [4] and [5] yield significantly better invisibility than those based on standard transformation optics. Indeed, we show that the newly proposed cloaks are sufficiently stable with respect to their basic features (values of the parameters and width of the layers).

When considering near cloaking for the Helmholtz equation, we prove that it becomes increasingly difficult as the cloaked object becomes bigger or the operating frequency becomes higher. The difficulty scales inversely proportionally to the object diameter or the frequency. Another important observation is that the reduction factor of the scattering cross section is higher in the backscattering region than in the forward one. This is due to the creeping waves propagating in the shadow region. We show that the cloaking problem becomes easier if only scattered waves at certain angles are visible.

Finally, we extend our construction to the enhanced reshaping problem. We show how to make any target look like a disc with homogeneous physical parameters.

2 Enhancement of near cloaking in the quasi-static limit

2.1 Principles

To explain the principle of our new construction of cloaking structures, we review the results on the conductivity equation obtained in [4].

Let Ω be a domain in $\mathbb{R}^2$ containing 0 possibly with multiple components with Lipschitz boundary. For a given harmonic function H in $\mathbb{R}^2$, consider

$$\begin{cases} \nabla\cdot\Big(\sigma_0\chi(\mathbb{R}^2\setminus\overline{\Omega})+\sigma\chi(\Omega)\Big)\nabla u=0 \quad \text{in } \mathbb{R}^2,\\ u(\mathbf{x})-H(\mathbf{x})=O(|\mathbf{x}|^{-1}) \quad \text{as } |\mathbf{x}|\to\infty, \end{cases} \tag{2.1}$$

where σ_0 and σ are conductivities (positive constants) of $\mathbb{R}^2\setminus\overline{\Omega}$ and Ω, respectively. Here and throughout this paper, $\chi(\Omega)$ (resp. $\chi(\mathbb{R}^2\setminus\overline{\Omega})$) is the characteristic function of Ω (resp. $\chi(\mathbb{R}^2\setminus\overline{\Omega})$).

If the harmonic function H admits the expansion

$$H(\mathbf{x})=H(0)+\sum_{n=1}^{\infty} r^n\big(a_n^c(H)\cos n\theta+a_n^s(H)\sin n\theta\big)$$

with $\mathbf{x}=(r\cos\theta, r\sin\theta)$, then we have the following formula

$$\begin{aligned}(u-H)(\mathbf{x})=&-\sum_{m=1}^{\infty}\frac{\cos m\theta}{2\pi m r^m}\sum_{n=1}^{\infty}\big(M_{mn}^{cc}a_n^c(H)+M_{mn}^{cs}a_n^s(H)\big)\\ &-\sum_{m=1}^{\infty}\frac{\sin m\theta}{2\pi m r^m}\sum_{n=1}^{\infty}\big(M_{mn}^{sc}a_n^c(H)+M_{mn}^{ss}a_n^s(H)\big) \quad \text{as } |\mathbf{x}|\to\infty.\end{aligned} \tag{2.2}$$

The coefficients $M_{mn}^{cc}, M_{mn}^{cs}, M_{mn}^{sc}$, and M_{mn}^{sc} are called the contracted generalized polarization tensors.

In [4], we have constructed structures with vanishing contracted generalized polarization tensors for all $|n|,|m|\le N$. We call such structures GPT-vanishing structures of order N. For doing so, we use a disc with multiple coatings. Let Ω be a disc of radius r_1. For a positive integer N, let $0<r_{N+1}<r_N<\ldots<r_1$ and define

$$A_j:=\{r_{j+1}<r=|\mathbf{x}|\le r_j\},\quad j=1,2,\ldots,N. \tag{2.3}$$

Let $A_0=\mathbb{R}^2\setminus\overline{\Omega}$ and $A_{N+1}=\{r\le r_{N+1}\}$. Set σ_j to be the conductivity of A_j for $j=1,2,\ldots,N+1$, and $\sigma_0=1$. Let

$$\sigma=\sum_{j=0}^{N+1}\sigma_j\chi(A_j). \tag{2.4}$$

Because of the symmetry of the disc, one can easily see that

$$M_{mn}^{cs}[\sigma]=M_{mn}^{sc}[\sigma]=0 \quad \text{for all } m,n, \tag{2.5}$$

$$M_{mn}^{cc}[\sigma]=M_{mn}^{ss}[\sigma]=0 \quad \text{if } m\ne n, \tag{2.6}$$

and

$$M_{nn}^{cc}[\sigma]=M_{nn}^{ss}[\sigma] \quad \text{for all } n. \tag{2.7}$$

Let $M_n=M_{nn}^{cc}$, $n=1,2,\ldots$, for the simplicity of notation. Let

$$\zeta_j:=\frac{\sigma_j-\sigma_{j-1}}{\sigma_j+\sigma_{j-1}},\quad j=1,\ldots,N+1. \tag{2.8}$$

The following is a characterization of GPT-vanishing structures. See [4].

Proposition 2.1 *If there are non-zero constants $\zeta_1,\ldots,\zeta_{N+1}$ ($|\zeta_j|<1$) and $r_1>\ldots>r_{N+1}>0$ such that*

$$\prod_{j=1}^{N+1}\begin{bmatrix}1 & \zeta_j r_j^{-2l}\\ \zeta_j r_j^{2l} & 1\end{bmatrix} \text{ is an upper triangular matrix for } l=1,2,\ldots,N, \tag{2.9}$$

then (Ω,σ), given by (2.3), (2.4), and (2.8), is a GPT-vanishing structure of order N, i.e., $M_l = 0$ for $l \le N$. More generally, if there are non-zero constants $\zeta_1, \zeta_2, \zeta_3, \dots$ ($|\zeta_j| < 1$) and $r_1 > r_2 > r_3 > \dots$ such that r_n converges to a positive number, say $r_\infty > 0$, and

$$\prod_{j=1}^{\infty} \begin{bmatrix} 1 & \zeta_j r_j^{-2l} \\ \zeta_j r_j^{2l} & 1 \end{bmatrix} \text{ is an upper triangular matrix for every } l, \tag{2.10}$$

then (Ω,σ), given by (2.3), (2.4), and (2.8), is a GPT-vanishing structure with $M_l = 0$ for all l.

Let (Ω,σ) be a GPT-vanishing structure of order N of the form (2.4). We take $r_1 = 2$ so that Ω is the disk of radius 2, and $r_{N+1} = 1$. We assume that $\sigma_{N+1} = 0$ which amounts to that the structure is insulated along ∂B_1. For small $\rho > 0$, let

$$\Psi_{\frac{1}{\rho}}(\mathbf{x}) = \frac{1}{\rho}\mathbf{x}, \quad \mathbf{x} \in \mathbb{R}^2. \tag{2.11}$$

Then, $(B_{2\rho}, \sigma \circ \Psi_{\frac{1}{\rho}})$ is a GPT-vanishing structure of order N and it is insulated on ∂B_ρ.

For a given domain Ω and a subdomain $B \subset \Omega$, we introduce the DtN map $\Lambda_{\Omega,B}[\sigma]$ as

$$\Lambda_{\Omega,B}[\sigma](f) = \sigma \frac{\partial u}{\partial \nu}\Big|_{\partial\Omega} \tag{2.12}$$

where u is the solution to

$$\begin{cases} \nabla \cdot \sigma \nabla u = 0 & \text{in } \Omega \setminus \overline{B}, \\ \dfrac{\partial u}{\partial \nu} = 0 & \text{on } \partial B, \\ u = f & \text{on } \partial\Omega \end{cases} \tag{2.13}$$

where ν is the outward normal to ∂B. Note that with $\Omega = B_2$, $\Lambda_{\Omega,B_\rho}[\sigma \circ \Psi_{\frac{1}{\rho}}]$ may be regarded as small perturbation of $\Lambda_{\Omega,\emptyset}[1]$. In fact, a complete asymptotic expansion of $\Lambda_{\Omega,B_\rho}[\sigma \circ \Psi_{\frac{1}{\rho}}]$ as $\rho \to 0$ is obtained and it is proved that

$$\left\| \Lambda_{\Omega,B_\rho}\left[\sigma \circ \Psi_{\frac{1}{\rho}}\right] - \Lambda_{B_2,\emptyset}[1] \right\| \le C\rho^{2N+2}$$

for some constant C independent of ρ, where the norm is the operator norm from $H^{1/2}(\partial\Omega)$ into $H^{-1/2}(\partial\Omega)$. We then push forward $\sigma \circ \Psi_{\frac{1}{\rho}}$ by the change of variables F_ρ,

$$F_\rho(\mathbf{x}) := \begin{cases} \left(\dfrac{3-4\rho}{2(1-\rho)} + \dfrac{1}{4(1-\rho)}|\mathbf{x}|\right)\dfrac{\mathbf{x}}{|\mathbf{x}|} & \text{for } 2\rho \le |\mathbf{x}| \le 2, \\ \left(\dfrac{1}{2} + \dfrac{1}{2\rho}|\mathbf{x}|\right)\dfrac{\mathbf{x}}{|\mathbf{x}|} & \text{for } \rho \le |\mathbf{x}| \le 2\rho, \\ \dfrac{\mathbf{x}}{\rho} & \text{for } |\mathbf{x}| \le \rho, \end{cases} \tag{2.14}$$

in other words,

$$(F_\rho)_*(\sigma \circ \Psi_{\frac{1}{\rho}}) = \frac{(DF_\rho)(\sigma \circ \Psi_{\frac{1}{\rho}})(DF_\rho)^T}{|\det(DF_\rho)|} \circ F_\rho^{-1}. \tag{2.15}$$

Note that F_ρ maps $|\mathbf{x}| = \rho$ onto $|\mathbf{x}| = 1$, and is the identity on $|\mathbf{x}| = 2$. So by invariance of DtN map, we have

$$\Lambda_{B_2,B_1}\left[(F_\rho)_*(\sigma \circ \Psi_{\frac{1}{\rho}})\right] = \Lambda_{B_2,B_\rho}\left[\sigma \circ \Psi_{\frac{1}{\rho}}\right] \tag{2.16}$$

Thus we obtain the following theorem, which shows that using GPT-vanishing structures we achieve enhanced near-cloaking.

Theorem 2.2 *([4]) Let the conductivity profile σ be a GPT-vanishing structure of order N such that $\sigma_{N+1} = 0$. There exists a constant C independent of ρ such that*

$$\left\| \Lambda_{B_2,B_1}\left[(F_\rho)_*(\sigma \circ \Psi_{\frac{1}{\rho}})\right] - \Lambda_{B_2,\emptyset}[1] \right\| \le C\rho^{2N+2}. \tag{2.17}$$

2.2 Performances

The purpose of this section is to compare through numerical computations the cloaking effect of the near cloaking of Kohn *et al* [14] and the enhanced near cloaking proposed in [4] and reviewed in the previous subsection. The comparison is done by means of the eigenvalues of the DtN maps $\Lambda_{B_2,B_1}\left[(F_\rho)_*(1)\right]$ and $\Lambda_{B_2,B_1}[(F_\rho)_*(\sigma\circ\Psi_{\frac{1}{\rho}})]$ where F_ρ is the diffeomorphism defined by (2.14) and σ is the GPT-vanishing structure of order N as defined in (2.4). The first one is the DtN map of the near cloaking structure and the latter one is that of the enhanced near cloaking structure. We assume that the core is insulated, namely, $\sigma_{N+1}=0$ for the GPT-vanishing structure σ of order N.

Recall from [4] that

$$\Big(\Lambda_{B_2,B_1}[(F_\rho)_*(\sigma\circ\Psi_{\frac{1}{\rho}})]-\Lambda_{B_2,\emptyset}[1]\Big)(e^{\pm ik\theta})=\frac{k\rho^{2k}M_k[\sigma]}{\pi k 2^{-2k+1}-M_k[\sigma]\rho^{2k}}e^{\pm ik\theta},\quad k\in\mathbb{N},\tag{2.18}$$

where $M_k[\sigma]$ is the condensed GPT of order N associated with the structure σ. It is worth emphasizing that here we used (2.16). In particular, one can see that

$$\Big(\Lambda_{B_2,B_1}[(F_\rho)_*(1)]-\Lambda_{B_2,\emptyset}[1]\Big)(e^{\pm ik\theta})=-\frac{k}{2}\frac{2(\frac{\rho}{2})^{2k}}{1+(\frac{\rho}{2})^{2k}}e^{\pm ik\theta},\quad k\in\mathbb{N}.\tag{2.19}$$

Let λ^k, $j=1,2,\ldots$, be the eigenvalues of $\Lambda_{B_2,\emptyset}[1]$ in decreasing order. Let $\lambda^k_{\rm WC}$, $\lambda^k_{\rm NC}$ and $\lambda^k_{\rm EC}$ be the eigenvalues (in decreasing order) of $\Lambda_{B_2,B_1}[1]$, $\Lambda_{B_2,B_1}[(F_\rho)_*(1)]$ and $\Lambda_{B_2,B_1}[(F_\rho)_*(\sigma\circ\Psi_{\frac{1}{\rho}})]$, respectively. (WC, NC and EC stand for 'Without Cloaking', 'Near Cloaking' and 'Enhanced Cloaking', respectively.) Here $\Lambda_{B_2,B_1}[1]$ is the DtN map where the conductivity of the annulus $B_2\setminus B_1$ is 1 and the core B_1 is insulated.

One can compute λ^k and $\lambda^k_{\rm WC}$ explicitly, and $\lambda^k_{\rm NC}$ using (2.19). The computation of $\lambda^k_{\rm EC}$ using (2.18) requires an explicit form of σ, which is quite difficult if N is large. So we compute it numerically. For that we use the GPT-vanishing structure of order N for $N=1,\ldots,6$, which was computed numerically in [4]. Figure 2.1 shows the results of computation when $N=3$ and 6. We emphasize that the conductivity fluctuates on coatings near the core. When $N=3$, the maximal conductivity is 5.5158 and the minimum conductivity is 0.4264; When $N=6$, they are 11.6836 and 0.1706.

Figure 2.2 shows the $\log_{10}$ of $(1,1)$-entry of the conductivities (matrices) obtained by applying the transform (2.15) to cloaking structures, *i.e.*, $\log_{10}((F_\rho)_*(\sigma\circ\Psi_{\frac{1}{\rho}}))_{11}$ for different N. The structures for different values of N are quite similar. They are obtained by segmenting the structure for $N=0$ into concentric layers and multiplying the anisotropic conductivity in each layer by the corresponding value in the conductivity profile of the GPT-vanishing structure.

Figure 2.3 shows the $\log_{10}$ of the discrepancies of the eigenvalues of the DtN maps for different structures. The black line represents $\log_{10}|\lambda^k_{\rm WC}-\lambda^k|$, the blue one $\log_{10}|\lambda^k_{\rm NC}-\lambda^k|$, and the other colored ones $\log_{10}|\lambda^k_{\rm EC}-\lambda^k|$ when GPT-vanishing structures of order $N=1,\ldots,6$ are used. We observe, in accordance with (2.19), the quasi-geometric discrepancy of the perturbation triggered by a hole with ratio $\left(\frac{\rho}{2}\right)^2$. We also see that the DtN associated with the GPT-vanishing cloaking structure of order N has almost the same first N eigenvalues as the one for homogeneous background with conductivity 1. Moreover, GPT-vanishing structures are much less visible than those obtained by the blow-up of an uncoated small hole. Note that the $\sup_k|\lambda^k_{\rm NC}-\lambda^k|$ is reached at $k=1$ for the near cloaking (perturbation of eigenvalues is non-increasing) and at $k=N+1$ when a GPT-vanishing structure of order N is used.

Another important remark is in connection with [23], where the anisotropic conductivity of the cloaking structure is segmented into concentric isotropic homogeneous coatings. By optimizing the thickness and material parameters of the isotropic layers, one can achieve a good invisibility performance. From a homogenization point of view, this construction is intriguing. In view of

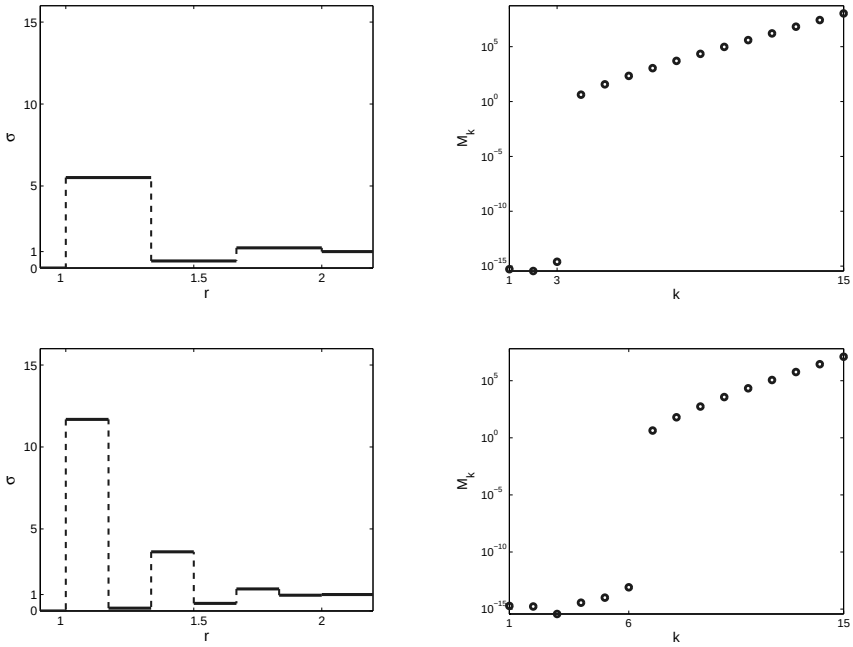

Figure 2.1: Conductivity profile (left) and GPTs (right) of the GPT-vanishing structure of order N with the core conductivity being 0. The first row is when $N = 3$ and the second one for $N = 6$.

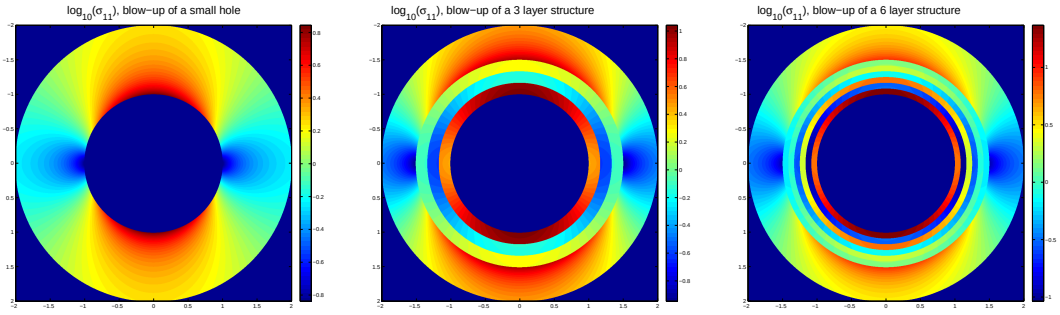

Figure 2.2: $\log_{10}$ of $(1,1)$-entry of the conductivities (matrices) obtained by applying the transform (2.15) to the GPT-vanishing structures of different N: $N = 0, 3, 6$ from left to right. $N = 0$ means no coating.

the discussion below, it seems that such a constructing using concentric isotropic layers (rank one structures in homogenization) is an approximation of the anisotropic conductivity in the sense that it minimizes the relative discrepancy between the DtN maps for only the first eigenvectors. The formalization of this new approximate homogenization concept will be the subject of a forthcoming work.

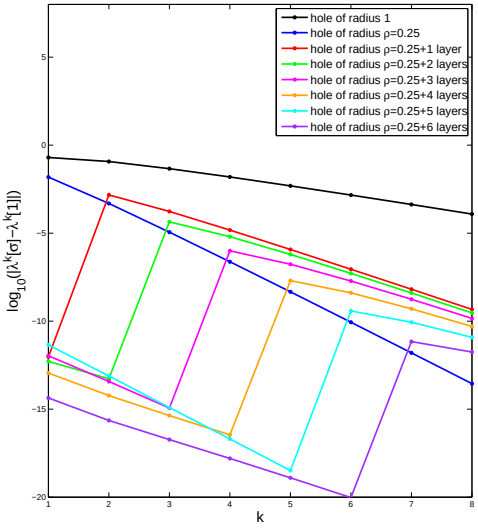

Figure 2.3: Perturbations of the eigenvalues of the DtN map. The black line is for $\log_{10}|\lambda^k_{\mathrm{WC}}-\lambda^k|$, the blue one for $\log_{10}|\lambda^k_{\mathrm{NC}}-\lambda^k|$, and the other colored ones for $\log_{10}|\lambda^k_{\mathrm{EC}}-\lambda^k|$ for $N=1,\ldots,6$.

2.2.1 Comparison of invisibility

Based on previous observation, we introduce, for small ρ, the following measure of the invisibility of a cloak: for a GPT vanishing structure σ of order N, let

$$\beta^N_{\mathrm{EC}}(\rho) := \sup_k |\lambda^k_{\mathrm{EC}}-\lambda^k|. \tag{2.20}$$

It is worth emphasizing that λ^k_{EC} depends on the radius ρ since it is an eigenvalue of $\Lambda_{B_2,B_1}[(F_\rho)_*(\sigma\circ\Psi_{\frac{1}{\rho}})]$. For a given ρ, let

$$\beta_{\mathrm{NC}}(\rho) := \sup_k |\lambda^k_{\mathrm{NC}}-\lambda^k|. \tag{2.21}$$

The measures of invisibility $\beta_{\mathrm{NC}}(\rho)$ and $\beta^N_{\mathrm{EC}}(\rho)$ are the largest perturbation due to the cloaking structure of the eigenvalues of the DtN map when the hole of radius ρ is used for the near cloaking and the enhanced near cloaking, respectively. We note that $\beta_{\mathrm{NC}}(\rho)$ is achieved when $k=1$ as (2.19) shows.

To achieve invisibility without using layers (near cloaking) which is equivalent to the enhanced cloaking of order N with the radius ρ, one has to use the hole of radius $\rho_{eq}(N)$ such that

$$\beta_{\mathrm{NC}}(\rho_{eq}(N)) = \beta^N_{\mathrm{EC}}(\rho). \tag{2.22}$$

One can see from (2.19) that

$$\rho_{eq}(N) = 2\sqrt{\frac{\beta^N_{\mathrm{EC}}(\rho)}{1-\beta^N_{\mathrm{EC}}(\rho)}}. \tag{2.23}$$

To obtain the same invisibility as a multi-coated structure of order 6 with $\rho=0.25$ by using the near cloaking (without layers), one has to transform the hole of radius $\rho_{eq}\approx 1.5\times 10^{-6}$, which will result in a much more singular conductivity distribution.

2.2.2 Behavior with respect to noise in the conductivity values

In this section we study the stability of the proposed invisibility cloak with respect to errors on the conductivities of the coatings. The number of layers is fixed to be 6. First we perturb all values of the conductivity profile with a normal error of standard deviation proportional to the value:

$$\sigma_j^{per} \equiv \sigma_j(1 + \mathcal{N}(0, \eta^2)), \quad j = 1, \ldots, N,$$

with $\eta \in [0,\ 0.5]$. For each noise level, 5000 realizations are drawn and the corresponding invisibility measure is computed.

Mean and standard deviation of the invisibility measure of the perturbed cloaks are plotted in Figure 2.4 as a function of noise level.

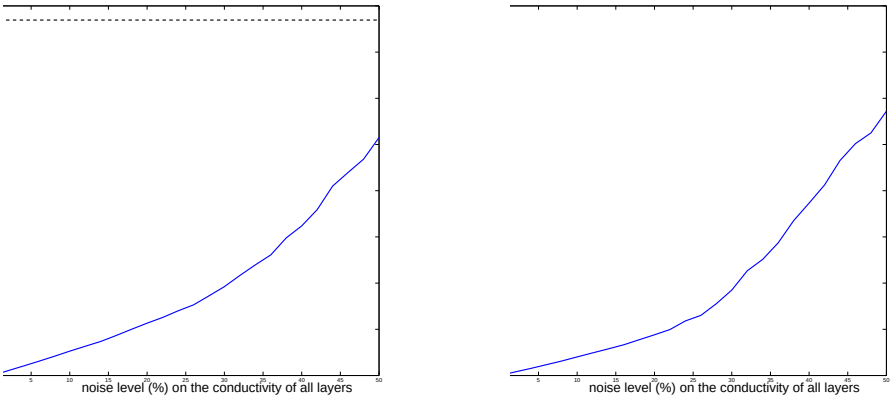

Figure 2.4: Mean and standard deviation of the invisibility measure as function of the noise level: the conductivity values are simultaneously perturbed. In dot is the visibility of the near cloaking (without layers) for $\rho = 0.25$.

High values of the standard deviation for high noise levels may cause some problems. While most of the realizations remain invisible (low mean value), a few ones may get quite visible.
We then perturb the value in each layer j_0 individually keeping the others at their correct values:

$$\sigma_{j_0}^{per} = \sigma_{j_0}(1 + \mathcal{N}(0, \eta^2)), \quad \sigma_j^{per} = \sigma_j,\ j \neq j_0.$$

Figure 2.5 shows that the most sensitive conductivity value is the one of the outermost layer.

We now perform a statistical sensitivity analysis of the invisibility measure using Sobol indices. The goal is to explain the fluctuations of the invisibility measure $\beta(\sigma_1, \ldots, \sigma_N)$ of the multi-layer cloak in terms of the conductivities $(\sigma_j)_{j=1}^N$. The problem can be formulated as $Y = f(\mathbf{X})$, where Y is a scalar output, the input $\mathbf{X}$ is a vector of random variables, and f is a deterministic but complex function. The Sobol indices are a set of nonnegative numbers that describe quantitatively the effects of the input variables [24, 25]. They are based on the decomposition of the variance of Y. See Appendix A.

In Figure 2.6 we choose all σ_i to be independent uniform random variables in the interval $[0.05, 5]$. Figure 2.6 shows that the values of the conductivities have a direct (not throughout their interaction) effect on the invisibility measure β_{EC}^N since the total indices are close to the first-order indices. Indeed, outer the layer higher its effect on the invisibility measure is.

In Figure 2.7 we choose the conductivities to be uniform fluctuations of the optimal conductivities which give invisibility. The mean values are chosen to be the optimal conductivity values and the variance is 0.1 times the optimal value.

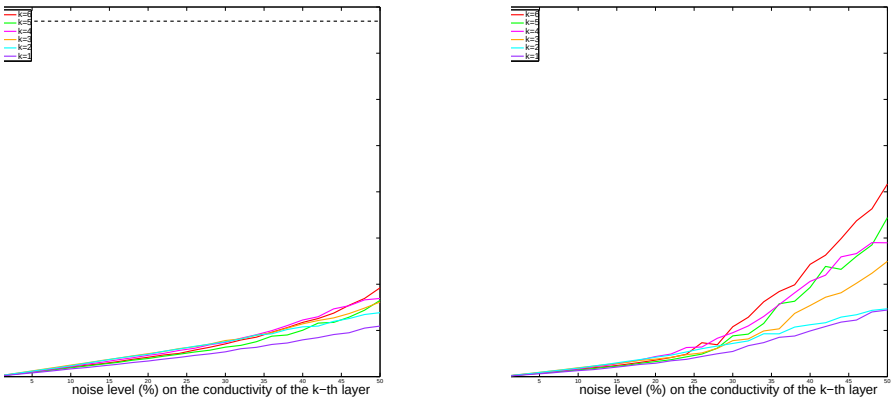

Figure 2.5: Mean and standard deviation of the invisibility measure as function of the noise level: the conductivity values are perturbed individually. In dot is the visibility of the near cloaking (without layers) for $\rho = 0.25$.

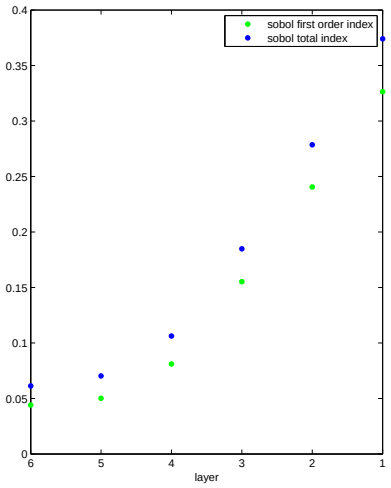

Figure 2.6: Sobol indices where the conductivities are chosen uniform random variables in the interval $[0.05, 5]$. Layer 1 is the outermost layer.

Figure 2.7 shows that around the optimal conductivity values, the interaction of the layers is very high since the total indices are much larger than the first-order indices. The layers affect the invisibility measure much more through their interaction than individually as in Figure 2.6. This is because of the high-nonlinearity of the invisibility measure in terms of the conductivities.

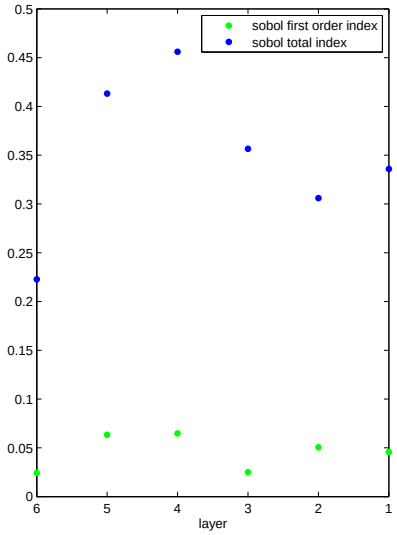

Figure 2.7: Sobol indices where the conductivities are chosen uniform random variables around the optimal values with relative variance equal to 0.1 the optimal values. Layer 1 is the outermost layer.

3 Enhancement of near cloaking for the Helmholtz equation

3.1 Principles

In this subsection we review the principles of the enhanced near cloaking by means of the far-field pattern or the scattering cross section for the Helmholtz equation, which was obtained in [5].

Let D be a bounded domain in $\mathbb{R}^2$ with Lipschitz boundary ∂D, and let (ϵ_0, μ_0) be the pair of electromagnetic parameters (permittivity and permeability) of $\mathbb{R}^2 \setminus \overline{D}$ and (ϵ_1, μ_1) be that of D. Then the permittivity and permeability distributions are given by

$$\epsilon = \epsilon_0 \chi(\mathbb{R}^2 \setminus \overline{D}) + \epsilon_1 \chi(D) \quad \text{and} \quad \mu = \mu_0 \chi(\mathbb{R}^2 \setminus \overline{D}) + \mu_1 \chi(D). \tag{3.1}$$

Given a frequency ω, set $k = \omega\sqrt{\epsilon_1 \mu_1}$ and $k_0 = \omega\sqrt{\epsilon_0 \mu_0}$. For a plane wave $e^{i\mathbf{k}\cdot\mathbf{x}}$, where $\mathbf{k} = k_0(\cos\theta_{\mathbf{k}}, \sin\theta_{\mathbf{k}})$, we consider the scattered wave u, *i.e.*, the solution to the following equation:

$$\begin{cases} \nabla \cdot \dfrac{1}{\mu} \nabla u + \omega^2 \epsilon u = 0 \quad \text{in } \mathbb{R}^2, \\ u - e^{i\mathbf{k}\cdot\mathbf{x}} \quad \text{satisfies the outgoing radiation condition.} \end{cases} \tag{3.2}$$

The far-field pattern $A_\infty[\epsilon, \mu, \omega]$ is defined to be

$$u(\mathbf{x}) - e^{i\mathbf{k}\cdot\mathbf{x}} = -ie^{-\frac{\pi i}{4}} \frac{e^{ik_0|\mathbf{x}|}}{\sqrt{8\pi k_0 |\mathbf{x}|}} A_\infty[\epsilon, \mu, \omega](\theta_{\mathbf{k}}, \theta_{\mathbf{x}}) + o(|\mathbf{x}|^{-\frac{1}{2}}) \quad \text{as } |\mathbf{x}| \to \infty. \tag{3.3}$$

Let $u_m, m \in \mathbb{Z}$, be the solution to the following equation:

$$\begin{cases} \nabla \cdot \dfrac{1}{\mu} \nabla u_m + \omega^2 \epsilon u_m = 0 \quad \text{in } \mathbb{R}^2, \\ u_m(\mathbf{x}) - J_m(k_0|\mathbf{x}|) e^{im\theta_{\mathbf{x}}} \quad \text{satisfies the outgoing radiation condition,} \end{cases} \tag{3.4}$$

where J_m is the Bessel function of order m. The scattering coefficients W_{nm}, $m, n \in \mathbb{Z}$, associated with the permittivity and permeability distributions ϵ, μ and the frequency ω are defined by

$$W_{nm} = W_{nm}[\epsilon, \mu, \omega] := \int_{\partial D} J_n(k_0|\mathbf{y}|)e^{-in\theta_{\mathbf{y}}}\psi_m(\mathbf{y})d\sigma(\mathbf{y}), \tag{3.5}$$

where $\psi_m \in L^2(\partial D)$ is the unique potential such that

$$u_m(\mathbf{x}) = J_m(k_0|\mathbf{x}|)e^{im\theta_{\mathbf{x}}} + \mathcal{S}_D^{k_0}[\psi](\mathbf{x}), \quad \mathbf{x} \in \mathbb{R}^2 \setminus \bar{D}. \tag{3.6}$$

Here $\mathcal{S}_D^{k_0}$ is the single layer potential defined by the fundamental solution to the operator $\Delta + k_0^2$. We refer to [5] for a precise definition of ψ_m.

The following proposition, which says that the scattering coefficients are basically the Fourier coefficients of the (doubly periodic) far-field pattern, holds.

Proposition 3.1 *Let θ and θ' be respectively the incident and scattered direction. Then we have*

$$A_\infty[\epsilon, \mu, \omega](\theta, \theta') = \sum_{n,m\in\mathbb{Z}} i^{(m-n)}e^{in\theta'}W_{nm}[\epsilon, \mu, \omega]e^{-im\theta}. \tag{3.7}$$

Moreover, the scattering cross section $S[\epsilon, \mu, \omega]$, defined by

$$S[\epsilon, \mu, \omega](\theta') := \int_0^{2\pi} \left|A_\infty[\epsilon, \mu, \omega](\theta, \theta')\right|^2 d\theta, \tag{3.8}$$

has the following representation in terms of the scattering coefficients W_{nm}:

$$S[\epsilon, \mu, \omega](\theta') = 2\pi \sum_{m\in\mathbb{Z}} \left| \sum_{n\in\mathbb{Z}} i^{-n}W_{nm}[\epsilon, \mu, \omega]e^{in\theta'} \right|^2. \tag{3.9}$$

Note that the optical theorem [6, 26] leads to a natural constraint on W_{nm}. In fact, we have

$$\Im m \sum_{n,m\in\mathbb{Z}} i^{m-n}e^{i(n-m)\theta'}W_{nm}[\epsilon, \mu, \omega] = -\sqrt{\frac{\pi\omega}{2}} \sum_{m\in\mathbb{Z}} \left| \sum_{n\in\mathbb{Z}} i^{-n}W_{nm}[\epsilon, \mu, \omega]e^{in\theta'} \right|^2, \quad \forall\, \theta' \in [0, 2\pi]. \tag{3.10}$$

In [5], we have designed a multi-coating around an insulated inclusion D, for which the scattering coefficients vanish. Such structures are transformed (by the transformation optics) to enhance near cloaking for the Helmholtz equation. Any target placed inside such structures will have nearly vanishing scattering cross section S, uniformly in the direction θ'. Let L be a positive integer. For positive numbers $r_1, \ldots, r_{L+1}$ with $2 = r_1 > r_2 > \cdots > r_{L+1} = 1$, let

$$A_j := \{x : r_{j+1} \le |\mathbf{x}| < r_j\}, \quad j = 1, \ldots, L, \quad A_0 := \mathbb{R}^2 \setminus \overline{A_1}, \quad A_{L+1}(= D) := \{\mathbf{x} : |\mathbf{x}| < 1\}.$$

Let (μ_j, ϵ_j) be the pair of permeability and permittivity of A_j for $j = 0, 1, \ldots, L+1$. Set $\mu_0 = 1$ and $\epsilon_0 = 1$. Let

$$\mu = \sum_{j=0}^{L+1} \mu_j\chi(A_j) \quad \text{and} \quad \epsilon = \sum_{j=0}^{L+1} \epsilon_j\chi(A_j). \tag{3.11}$$

Exactly like the quasi-static regime, one can show using symmetry that

$$W_{nm} = 0 \quad \text{if } m \neq n. \tag{3.12}$$

Let us define W_n by

$$W_n := W_{nn}. \tag{3.13}$$

Given L (the number of layers), the radii, $r_2, \ldots, r_L$, N, and ω, our purpose is to find, μ and ϵ so that $W_n[\mu, \epsilon, \rho\omega] = 0$ for $|n| \leq N$. Here ρ be a small parameter. We call such a structure (μ, ϵ) an *S-vanishing structure of order N at low-frequencies*. Such structure will be transformed by the change of variables (2.15) to a cloaking structure for all frequencies less than ω. Compared to the GPT-vanishing structure, we fix the radii of the layers and their number, and make the optimization over the material parameters. Note that, for the GPT-vanishing structure, the number of the layers is equal to the order of the structure. The following proposition was obtained in [5].

Proposition 3.2 *For $n \geq 1$, let W_n be defined by (3.13). We have*

$$W_n[\mu, \epsilon, t] = t^{2n} \left(W_n^0[\mu, \epsilon] + \sum_{l=1}^{(N-n)} \sum_{j=0}^{M_{n,l}} W_n^{l,j}[\mu, \epsilon] t^{2l} (\ln t)^j \right) + o(t^{2N}), \tag{3.14}$$

where $t = \rho\omega$, $M_{n,l} := (L+1)(N-n)$ (L being the number of layers), and the coefficients $W_n^0[\mu, \epsilon]$ and $W_n^{l,j}[\mu, \epsilon]$ are independent of t.

In view of Proposition 3.2, to construct an (semi-)S-vanishing structure of order N at low frequencies, we need to have a pair (μ, ϵ) of the form (3.11) satisfying

$$W_n^0[\mu, \epsilon] = 0, \text{ and } W_n^{l,j}[\mu, \epsilon] = 0 \quad \text{for } 0 \leq n \leq N,\ 1 \leq l \leq (N-n),\ 1 \leq j \leq M_{n,l}. \tag{3.15}$$

Such a structure can be reconstructed numerically for small N. The following theorem holds.

Theorem 3.3 *If (μ, ϵ) is an S-vanishing structure of order N at low frequencies, then there exists ρ_0 such that*

$$A_\infty \Big[(F_\rho)_*(\mu \circ \Psi_{\frac{1}{\rho}}), (F_\rho)_*(\epsilon \circ \Psi_{\frac{1}{\rho}}), \omega \Big](\theta, \theta') = o(\rho^{2N}), \tag{3.16}$$

and

$$S \Big[(F_\rho)_*(\mu \circ \Psi_{\frac{1}{\rho}}), (F_\rho)_*(\epsilon \circ \Psi_{\frac{1}{\rho}}), \omega \Big](\theta') = o(\rho^{4N}), \tag{3.17}$$

for all $\rho \leq \rho_0$, uniformly in θ and θ'.

Note the cloaking enhancement is achieved for all the frequencies smaller than ω.

3.2 Performances

A good scalar measure of the invisibility of a scatterer (for a given frequency) may be the maximum of the scattering cross-section:

$$\beta(\mu, \epsilon, \omega) = \sup_{\theta \in\ [0\ 2\pi]} S[\mu, \epsilon, \omega](\theta). \tag{3.18}$$

If we consider a discretization of the directions θ, θ' with N_θ values, then because of the behavior of the scattering coefficients W_n, only a few coefficients will be significantly non-zero. The vectors $e^{in\theta}$ (where $\theta = (\theta_1, \ldots, \theta_{N_\theta})$) are orthogonal (for $n \neq m$) in $L^2(]0, 2\pi[)$. Thus, from the expression (3.7) of the far-field pattern, the singular values of the discretized operator are given by

$$\sigma_j = N_\theta |W_{n(j)}|,$$

where $n(j)$ is just sorting the N_θ largest scattering coefficients. Hence, we have a direct correspondence between the scattering coefficients of the cloaking structure and the SVD of its far-field pattern. Note that symmetry implies $W_{-n} = W_n$, and we expect one singular value of multiplicity 1 (for $n = 0$) and a series of singular values with multiplicity 2.

3.2.1 Comparisons of the performance

We give in Figure 3.1 the (real part of the) outer full field u, the outer scattered field u_s (the field inside the cloak is not computed) and the scattering cross-section for the hole of unit radius with Neumann boundary conditions in the three following situations: uncloaked hole, usual near cloaking (with using layers), and 1 S-vanishing structure. The source wave is a plane wave in the direction [1 0] ($\theta = 0$) at frequency $\omega = \pi$ and $\rho = 0.05$. A few remarks are in order:

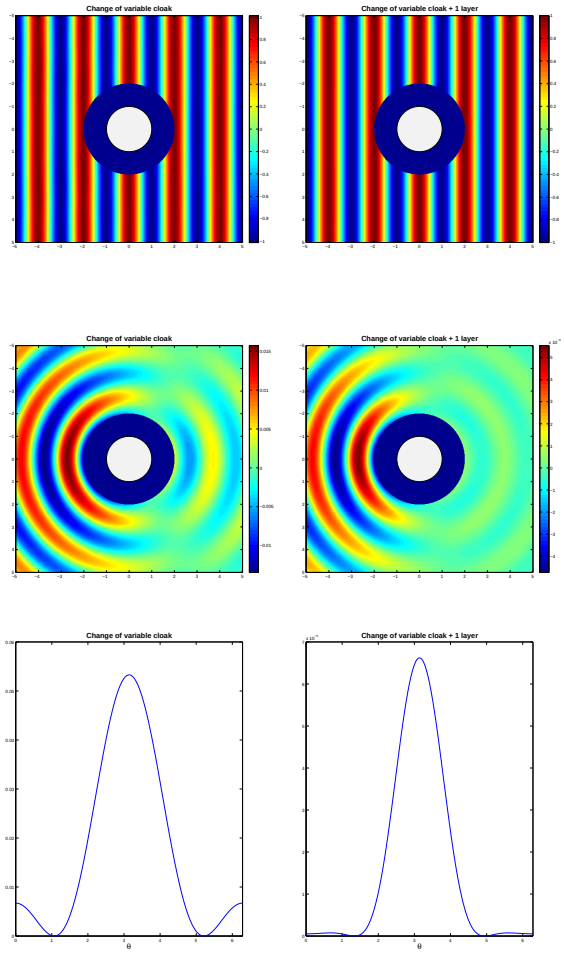

Figure 3.1: Top: outer full field; middle: outer scattered field; bottom: scattering cross-section; left: uncloaked hole; center: usual change of variables-based cloak; right: S-vanishing cloaking structure of order one.

- while the change of variables-based cloak shows good performance (it makes the hole with radius 1 looks like a hole with radius ρ), using an S-vanishing structure greatly improves invisibility. This can be seen by inspecting the second and third rows in Figure 3.1
- the uncloaked hole has stronger forward scattering (on the right), while the cloaked structures have stronger back-scattering (on the left). Actually, the cloaking structure reduces forward scattering with higher order than backscattering. This seems to happen because the hole is

of the size of the wavelength, thus leaves a shadow. The cloaked holes "appear" of size ρ which is much smaller than the wavelength $2\pi/\omega$ and act mostly as weak reflectors.

3.2.2 Behavior with respect to noise in the permeability and permittivity values

In this subsection we study stability of the proposed invisibility cloaks with respect to errors in the permeabilities and permittivities of the vanishing S-coefficients structure. The number of layers is fixed to be 1. First we perturb the permeability value with a normal error of standard deviation proportional to the value:

$$\mu_1^{per} = \mu_1(1 + \mathcal{N}(0, \eta^2))$$

with $\eta \in [0,\ 0.5]$. Mean and standard deviation of the invisibility measure, given by (3.18), of the perturbed cloaks are plotted in Figure 3.2 as a function of noise level. Then we perturb the

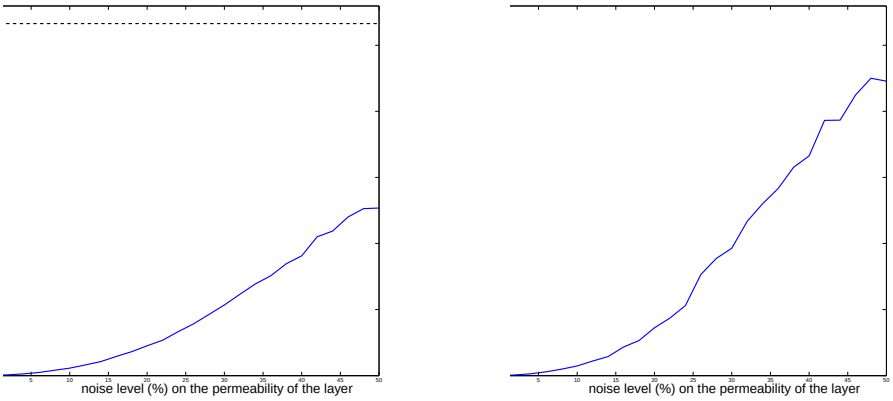

Figure 3.2: Mean and standard variation of the invisibility measure as function of the noise level in the permeability value. In dot is the visibility of the near cloaking (without layers) for $\rho = 0.05$.

permittivity value as follows

$$\epsilon_1^{per} = \epsilon_1(1 + \mathcal{N}(0, \eta^2))$$

with $\eta \in [0,\ 0.5]$. Mean and standard deviation of the visibility of the perturbed cloaks are plotted in Figure 3.3 as a function of noise level. As in the conductivity case, the most sensitive parameter values are those of the outermost layer.

3.3 Invisibility from limited-view measurements

In this subsection we consider the problem of designing a cloaking structure that makes any target placed inside it invisible to waves for certain incidence and/or scattered directions.

Assume in Proposition 3.1 that $\theta \in (-\phi_s, \phi_s)$ and $\theta' \in (\phi_c - \phi_i, \phi_c + \phi_i)$, where $0 < \phi_s, \phi_i < \pi$. Consider the multi-coated concentric disc structure. From (3.7), it follows that the scattering cross section $S[\epsilon, \mu, \omega]$ of the multi-coated structure has the following representation in terms of the scattering coefficients W_n:

$$\int_{\phi_c-\phi_i}^{\phi_c+\phi_i} S[\epsilon, \mu, \omega](\theta')\, d\theta' = \frac{4\pi^4}{\phi_i \phi_s} \sum_{n,l\in\mathbb{Z}} W_n \overline{W_l} \mathrm{sinc}(n-l)\phi_i\, \mathrm{sinc}(n-l)\phi_s\, e^{-i(n-l)\phi_c}. \tag{3.19}$$

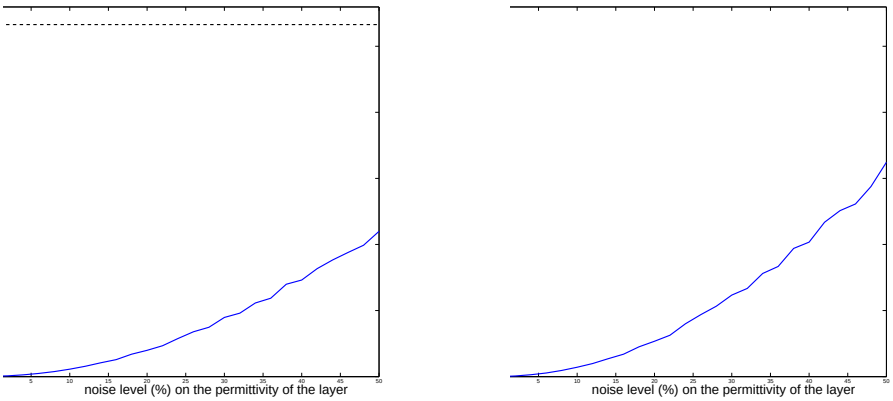

Figure 3.3: Mean and standard variation of the invisibility measure as function of the noise level in the permittivity value. In dot is the visibility of the near cloaking (without layers) for $\rho = 0.05$.

We contrast this with the full-aperture case ($\phi_s = \phi_i = \pi$), where $S[\epsilon, \mu, \omega](\theta')$ is given by

$$S[\epsilon, \mu, \omega](\theta') = 2\pi \sum_{n \in \mathbb{Z}} |W_n|^2$$

and is, by symmetry, independent of θ'. Therefore, in the limited-view case, in order to enhance the near cloaking, one should make the first coefficients in the Taylor expansion of

$$\sum_{n,l \in \mathbb{Z}} W_n[\mu, \epsilon, t]\overline{W_l}[\mu, \epsilon, t]\text{sinc}(n-l)\phi_i \text{sinc}(n-l)\phi_s e^{-i(n-l)\phi_c},$$

in terms of t equal zero. Compared to the full-aperture case, combinations of scattering coefficients are made to vanish.

3.4 Reshaping problem

In this subsection we propose to use a construction similar to the one in the last section to generate a general illusion such that an arbitrary target appears to be like some other object of our choice from scattering cross-section measurements. For simplicity, we take the object to be B_2 with given constant electromagnetic parameters ϵ_2, μ_2. Inside B_2 we place a small hole ρB_1. It is known that ρB_1 has a small effect on the scattering cross-section measurements. Now, using the transformation optics, we push forward ρB_1 to B_1 keeping the boundary ∂B_2 invariant. The obtained electromagnetic distributions in $B_2 \setminus \overline{B_1}$ are anisotropic and any target placed inside B_1 has the same scattering cross-section than B_2 with electromagnetic parameters ϵ_2, μ_2. In order to enhance the illusion effect, one can extend the idea of multi-coating. Here, we construct the concentric disc structure in exactly the same manner as in the previous subsection but taking in A_0 (ϵ_2, μ_2) to be the pair of electromagnetic parameters instead of $(1, 1)$.

4 Concluding remarks

The numerical stability study we presented is conclusive but some aspects may be improved.

First, the noise acts on variables in the virtual space $B_2 \setminus \overline{\rho B_1}$ (*i.e.*, before applying transformation optics). Indeed, the perturbed profiles (conductivity, permeability, permittivity) are in this virtual space. To get in the real space, $B_2 \setminus \overline{B_1}$, we have to compose them with the (anisotropic, non-radially symmetric) change of variables. What we study is then the effect of an error (or an approximation) in the algorithm to get the profile. It could also be practical and interesting to study the effects of errors in the realization of the physical cloaks. The second point is that the study is purely numeric. It would be interesting to better understand the functions that gives the contracted GPTs (or the scattering coefficients) in terms of the material parameters and then to show that a small variation in the material parameters results in a small variation in the contracted GPTs (or the scattering coefficients), and thus in the invisibility. In other words, we have to show that the function is at the very least locally convex around its local minima. Figure 4.1 shows such a function for a 2-layer structure in the quasi-static limit.

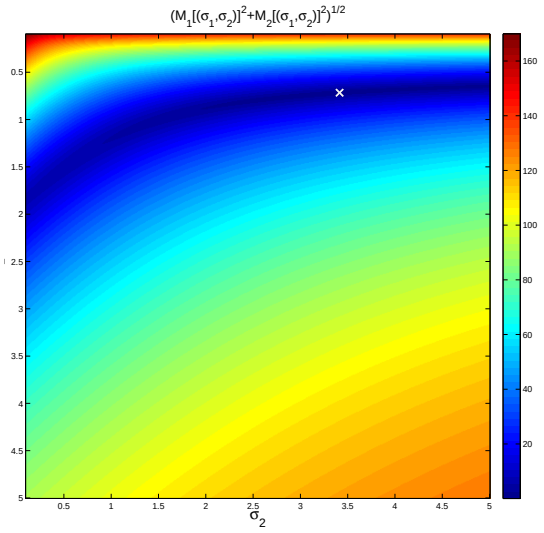

Figure 4.1: The contracted GPTs of a two-layered structure as a function of the material parameters.

The white $\times$ is the value we get with the algorithm. Figure 4.1 confirms the numerical observation that the invisibility measure is more sensitive to σ_1 (the outermost value) than to σ_2.

Finally, since a GPT-vanishing structure has a stepwise constant conductivity $\sigma \circ \Psi_{\frac{1}{\rho}} \circ F_\rho^{-1}$, it would be interesting to try to replace each anisotropic layer of the cloaking structure by two equivalent isotropic layers as done in [23]. Using this idea we would end up with an isotropic radially symmetric conductivity. It would be interesting to see its invisibility performance.

A Statistical sensitivity analysis

The goal is to explain the fluctuations of a scalar output Y in terms of the input random variables $\mathbf{X}$, when they are related through a deterministic but complex function f: $Y = f(\mathbf{X})$. The Sobol indices are a set of nonnegative numbers that describe quantitatively the effects of the input variables. They are based on the decomposition of the variance of Y.

A.1 Sobol indices

Let us assume that the output is of the form $Y = f(X_1, \ldots, X_N)$ where f is a deterministic function and the input random variables are real-valued and independent. Then there exist functions such that the output can be written as

$$f(X_1, \ldots, X_N) = f_0 + \sum_{i=1}^{N} f_i(X_i) + \sum_{1 \le i < j \le N} f_{ij}(X_i, X_j) + \cdots + f_{1\ldots N}(X_1, \ldots, X_N), \qquad \text{(A.1)}$$

where

$$\mathbb{E}[f_{i_1\ldots i_s}(X_{i_1}, \ldots, X_{i_s}) f_{j_1\ldots j_t}(X_{j_1}, \ldots, X_{j_t})] = 0 \text{ if } (i_1 \ldots i_s) \neq (j_1 \ldots j_t).$$

In fact there is a unique solution to this problem which can be written in terms of the conditional expectations of Y:

$$\begin{aligned} f_0 &= \mathbb{E}[Y], \\ f_i(X_i) &= \mathbb{E}[Y|X_i] - f_0, \\ f_{ij}(X_i, X_j) &= \mathbb{E}[Y|X_i, X_j] - f_i(X_i) - f_j(X_j) - f_0, \\ &\vdots \end{aligned}$$

Using formula (A.1) the variance of Y, $D = \mathrm{Var}(Y)$, can be written as

$$D = \sum_{i=1}^{N} D_i + \sum_{1 \le i < j \le N} D_{ij} + \cdots + D_{1\ldots N},$$

where

$$\begin{aligned} D_i &= \mathrm{Var}\big(E[Y|X_i]\big), \\ D_{ij} &= \mathrm{Var}\big(E[Y|X_i, X_j] - E[Y|X_i] - E[Y|X_j]\big), \\ &\vdots \end{aligned}$$

The Sobol sensitivity indices are defined by

$$S_i = \frac{D_i}{D}, \qquad S_{ij} = \frac{D_{ij}}{D}, \quad \ldots.$$

Note that we have

$$S_i \ge 0, \qquad S_{ij} \ge 0, \quad \text{and} \quad \sum_{i=1}^{N} S_i + \sum_{1 \le i < j \le d} S_{ij} + \cdots + S_{1\ldots N} = 1.$$

We can interpret the indices as follows:

- S_i is the first-order index. It explains the part of the variance of Y that can be explained by the fluctuations of X_i.
- S_{ij} is the second-order index. It explains the part of the variance of Y that can be explained by the interaction of the fluctuations of the variables X_i and X_j.
- The total number of Sobol indices is $2^N - 1$, which can be large and which makes the sensitivity analysis not easy to interpret. One then introduces the N total sensitivity indices

$$S_{Ti} = \text{ sum of all indices relative to } X_i = \sum_{p=1}^{N} \sum_{\{i\} \subset (j_1 \ldots j_p)} S_{j_1\ldots j_p},$$

  which expresses the sensitivity of Y with respect to X_i by itself or through its interactions with other variables.

In practice one computes the first-order indices S_i and the total indices S_{Ti} for $i = 1, \ldots, N$.
- If S_{Ti} is small, then this means that the variable X_i has negligible effect.
- If S_i is large then this means that the variable X_i has important effect by itself.
- If S_i is small and S_{Ti} is large, then this means that the variable X_i has important effects but only through its interaction with other variables.

A.2 Monte Carlo estimation of the Sobol indices

The first-order index is

$$S_i = \frac{D_i}{D} = \frac{\mathrm{Var}(E[Y|X_i])}{\mathrm{Var}(Y)}.$$

The mean $f_0 = \mathbb{E}[Y]$ and variance $D = \mathrm{Var}(Y)$ can be estimated by

$$\begin{aligned} \widehat{f_0} &= \frac{1}{n}\sum_{k=1}^{n} f(X_1^{(k)}, \ldots, X_{i-1}^{(k)}, X_i^{(k)}, X_{i+1}^{(k)}, \ldots, X_N^{(k)}), \\ \widehat{D} &= \frac{1}{n}\sum_{k=1}^{n} f(X_1^{(k)}, ..., X_{i-1}^{(k)}, X_i^{(k)}, X_{i+1}^{(k)}, \ldots, X_N^{(k)})^2 - \widehat{f}_0^2, \end{aligned}$$

where $(X_1^{(k)}, \ldots, X_N^{(k)})_{k=1\ldots n}$ is a sample of size n of the input variables.

$D_i = \mathrm{Var}(E[Y|X_i])$ can be estimated by

$$\widehat{D}_i = \frac{1}{n}\sum_{k=1}^{n} f(X_1^{(k)}, \ldots, X_{i-1}^{(k)}, X_i^{(k)}, X_{i+1}^{(k)}, \ldots, X_N^{(k)}) f(\widetilde{X}_1^{(k)}, \ldots, \widetilde{X}_{i-1}^{(k)}, X_i^{(k)}, \widetilde{X}_{i+1}^{(k)}, \ldots, \widetilde{X}_N^{(k)}) - \widehat{f}_0^2,$$

where $(\widetilde{X}_1^{(k)}, \ldots, \widetilde{X}_N^{(k)})_{k=1\ldots n}$ is a second sample of the input variables (independent of the first one).

The total sensitivity index is

$$S_{Ti} = \frac{\widetilde{D}_i}{D}, \qquad \widetilde{D}_i = \sum_{p=1}^{N} \sum_{\{i\} \subset (j_1 \ldots j_p)} D_{j_1 \ldots j_p}.$$

Using the same two samples as above, $\widetilde{D}_i$ can estimated by

$$\widehat{\widetilde{D}}_i = \frac{1}{n}\sum_{k=1}^{n} f(X_1^{(k)}, \ldots, X_{i-1}^{(k)}, X_i^{(k)}, X_{i+1}^{(k)}, \ldots, X_N^{(k)}) f(X_1^{(k)}, \ldots, X_{i-1}^{(k)}, \widetilde{X}_i^{(k)}, X_{i+1}^{(k)}, \ldots, X_N^{(k)}) - \widehat{f}_0^2.$$

References

[1] A. Alú and N. Engheta, Achieving transparency with plasmonic and metamaterial coatings, Phys. Rev. E., 72 (2005), 106623, 9 pp.

[2] H. Ammari, G. Ciraolo, H. Kang, H. Lee, and G. Milton, Spectral theory of a Neumann-Poincaré-type operator and analysis of cloaking due to anomalous localized resonance, submitted.

[3] H. Ammari and H. Kang, *Polarization and Moment Tensors with Applications to Inverse Problems and Effective Medium Theory*, Applied Mathematical Sciences, Vol. 162, Springer-Verlag, New York, 2007.

[4] H. Ammari, H. Kang, H. Lee, and M. Lim, Enhancement of near cloaking using generalized polarization tensors vanishing structures. Part I: the conductivity problem, submitted.

[5] H. Ammari, H. Kang, H. Lee, and M. Lim, Enhancement of near cloaking. Part II: the Helmholtz equation, submitted.

[6] M. Born and E. Wolf, *Principles of Optics: Electromagnetic Theory of Propagation, Interference and Diffraction of Light*, Cambridge University Press, 6 edition, Cambridge, 1997.

[7] G. Bouchitté and B. Schweizer, Cloaking of small objects by anomalous localized resonance, Quart. J. Mech. Appl. Math. 63 (2010), 437–463.

[8] O.P. Bruno and S. Lintner, Superlens-cloaking of small dielectric bodies in the quasi-static regime, J. Appl. Phys. 102 (2007), 124502.

[9] K. Bryan and T. Leise, Impedance Imaging, inverse problems, and Harry Potter's Cloak, SIAM Rev., 52 (2010), 359–377.

[10] A. Greenleaf, Y. Kurylev, M. Lassas, and G. Uhlmann, Cloaking devices, electromagnetic wormholes, and transformation optics, SIAM Rev., 51 (2009), 3–33.

[11] F. Guevara Vasquez and G. W. Milton and D. Onofrei, Broadband exterior cloaking, Opt. Express 17 (2009), 14800–14805.

[12] H. Hashemi, A. Oskooi, J. D. Joannopoulos, and S. G. Johnson, General scaling limitations of ground-plane and isolated-object cloaks, Phys. Rev. A, 84 (2011), 023815.

[13] R. V. Kohn, D. Onofrei, M. S. Vogelius, and M. I. Weinstein, Cloaking via change of variables for the Helmholtz equation, Comm. Pure Appl. Math., 63 (2010), 973–1016.

[14] R. V. Kohn, H. Shen, M. S. Vogelius, and M. I. Weinstein, Cloaking via change of variables in electric impedance tomography, Inverse Problems, 24 (2008), article 015016.

[15] U. Leonhardt, Optical conforming mapping, Science, 312 (2006), 5781, 1777–1780.

[16] U. Leonhardt and T. Tyc, Broadband invisibility by non-euclidean cloaking, Science, 323 (2009), 110–111.

[17] H. Liu, Virtual reshaping and invisibility in obstacle scattering, Inverse Problems, 25 (2009), 044006, 16 pp.

[18] D. A. B. Miller, On perfect cloaking, Optics Express, 14 (2006), 12457–12466.

[19] G. Milton and N. A. Nicorovici, On the cloaking effects associated with anomalous localized resonance, Proc. R. Soc. A 462 (2006), 3027-3059.

[20] G. Milton, N. A. Nicorovici, R. C. McPhedran, and V. A. Podolskiy, A proof of superlensing in the quasistatic regime, and limitations of superlenses in this regime due to anomalous localized resonance, Proc. R. Soc. A 461 (2005), 3999-4034.

[21] H. M. Nguyen, Cloaking via change of variables for the Helmholtz equation in the whole space, Comm. Pure Appl. Math., 63 (2010), 1505–1524.

[22] J. B. Pendry, D. Schurig, and D. R. Smith, Controlling electromagnetic fields, Science, 312 (2006), 1780–1782.

[23] C. W. Qiu, L. Hu, B. Zhang, B.-I. Wu, S. G. Johnson, and J. D. Joannopoulos, Spherical cloaking using nonlinear transformations for improved segmentation into concentric isotropic coatings, Optics Express, 17 (2009), 13467–13478.

[24] A. Saltelli, K. Chan, and E. M. Scott, *Sensitivity Analysis*, Wiley, Wichester, 2000.

[25] I. M. Sobol, Sensitivity estimates for nonlinear mathematical models, Math. Model. Comput. Exp., 1 (1993), 407–414.

[26] M. E. Taylor, *Partial Differential Equations II. Qualitative Studies of Linear Equations*, Appl. Math. Sci., Vol. 116, Springer-Verlag, New York, 1996.

[27] Y. A. Urzhumov, N. B. Kundtz, D. R. Smith, and J. B. Pendry, Cross-section comparisons of cloaks designed by transformation optical and optical conformal mapping approaches, J. Opt., 13 (2011), 024002.